Published in: Biomaterials (2001), vol. 22, iss. 10, pp. 1137-1146
Status: Postprint (Author's version)

Poly(D,L-lactide) foams modified by poly(ethylene oxide)-block-poly(D,L-lactide) copolymers and a-FGF: in vitro and in vivo evaluation for spinal cord regeneration

V. Maquet[(1)], D. Martin[(2)], F. Scholtes[(3)], R. Franzen[(4)], J. Schoenen[(4)], G. Moonen[(3)], R. Jérôme[(1)]

[(1)]Center for Education and Research on Macromolecules, University of Liège, Institute of Chemistry, B6, Sart-Tilman, 4000 Liège, Belgium
[(2)]Department of Neurosurgery, CHU, University of Liège, Belgium
[(3)]Department of Human Physiology and Physiopathology, University of Liège, Belgium
[(4)]Department of Neuroanatomy, CHU, University of Liège, Belgium

Abstract
The first goal of this study was to examine the influence that poly(ethylene oxide)-block-poly(D,L-lactide) (PELA) copolymer can have on the wettability, the in vitro controlled delivery capability, and the degradation of poly(D,L-lactide) (PDLLA) foams. These foams were prepared by freeze-drying and contain micropores (10 μm) in addition of macropores (100 μm) organized longitudinally. Weight loss, water absorption, changes in molecular weight, polymolecularity *(M_w/M_n)* and glass transition temperature *(T_g)* of PDLLA foams mixed with various amounts of PELA were followed with time. It was found that 10 wt% of PELA increased the wettability and the degradation rate of the polymer foams. The release of sulforhodamine (SR) was compared for PDLLA and PDLLA-PELA foams in relation with the foam porosity. An initial burst release was observed only in the case of the 90:10 PDLLA/PELA foam. The ability of the foam of this composition to be integrated and to promote tissue repair and axonal regeneration in the transected rat spinal cord was investigated. After implantation of ca. 20 polymer rods assembled with fibrin-glue, the polymer construct was able to bridge the cord stumps by forming a permissive support for cellular migration, angiogenesis and axonal regrowth.

Keywords: Poly(D,L-lactide) porous supports; Poly(ethylene oxide)-block-poly(D,L-lactide) copolymer; Acidic fibroblast growth factor; In vitro degradation; Central nervous system; Spinal cord; Regeneration

1. Introduction

Poly(lactic acid) (PLA) is widely proposed for the manufacturing of three-dimensional polymer scaffolds for cell transplantation and tissue regeneration, because of biocompatibility, biodegradability and easy processa-bility. It is accepted that a polymer scaffold must be highly porous for a sufficient cell density to be seeded in vitro, for blood invasion to occur in vivo, and for oxygen and nutrients to be supplied to cells. We have developed a freeze-drying technique to produce PLA foams with high porosity and random or aligned pores [1,2]. We previously demonstrated that neuronal cells were able to survive and to support growth of axonal processes when cultured in vitro on foams with both types of pore morphology. However, we found that the foams were floating in the cell culture medium, due to the high hydrophobicity of PLA. In order to overcome this drawback, the PLA supports were coated by hy-drophilic polyvinylalcohol (PVA). PVA-coated PLA foams with a longitudinal network of macropores (diameter ≈ 100 μm) were further implanted in vivo between the two stumps of the transected rat sciatic nerve, where they proved able to support migration of cells, including Schwann cells, endothelial cells and phagocytes. They also allowed axonal regeneration from the proximal to the distal nerve segments [3]. Unexpectedly, cell migration and axogenesis were essentially localized at the outer surface of the polymer implant, suggesting that the porous surface was more favorable to axonal regrowth than the internal macropores. The fast release of the hydrophilic PVA coating from the polymer implant could explain, at least partially, this result. This paper reports a novel strategy to improve and sustain the wettability of the PLA foams by addition of an am-phiphilic block copolymer of lactide and ethylene oxide (PELA). The preparation of PDLLA/PELA foams, their wettability, their ability to release low molecular weight compounds and their degradability will be reported first. The question of whether injured axons can grow through these foams will then be addressed. For this purpose, ca. twenty porous polymer rods of a selected PDLLA-PELA mixture (10wt%) were implanted into a lesion of the spinal cord of adult rats, known for its poor spontaneous regenerative capacity.

2. Materials and methods

2.1. Materials

Poly(D,L-lactide) (PDLLA) [Resomer® R206] was supplied by Boehringer-Ingelheim. The PELA copolymer was synthesized by ring-opening polymerization of D,L-lactide from poly(ethylene oxide)-monomethylether (Me.PEO, M_w ca. ≈ 5000), supplied by Sigma. The selected PELA copolymer was of narrow molecular weight distribution (1.14) and contained a PLA block of 4300 molecular weight (M_n) as determined by ^{1}H-NMR spectroscopy. Sulforhodamine (SR) was purchased from Sigma.

2.2. PDLLA-PELA foams

Mixtures of PDLLA and PELA were prepared as follows: PDLLA was dissolved in dioxane at a concentration of 5 wt:vol%. The PELA was dissolved separately in chloroform and mixed with the PDLLA solution, so as to reach PELA proportions of 0, 1, 5, 10wt% with respect to PDLLA. The solution was frozen for 2h in liquid nitrogen, dried by vacuum sublimation for 48 h at -10°C, for 48 h at 0°C, and finally at room temperature until it reached a constant weight.
The morphology of the freeze-dried foams was observed by scanning electron microscopy (SEM, Jeol, JSM-840A). Surface and cross-section of the foams were coated with platinum and their morphology was examined at an accelerating voltage of 20 kV.

2.3. Loading and in vitro release of SR

PDLLA (A) and PDLLA-PELA (10%) (B) foams were loaded with SR by mixing 1% SR with the polymer solution prior to freeze-drying. Two mixing techniques were used for foam A, i.e. dispersion of SR as a solid powder (A_{dis}) and solubilization in water (A_{sol}). For foam B, only the technique where SR was solubilized in water and mixed to the organic solution (98/2 dioxane/water) was used (B_{sol}). The dispersion or the solution was poured into a lyophilization flask and frozen by immersion into liquid nitrogen for two hours. The conditions of lyophilization were the same as described above.
Disks (12 mm diameter) were cut out from 4-5 mm thick SR-loaded foams using a cork borer, and longitudinally sectioned in order to study the release of SR from both the surface (top layer) and the core (sublayer). Five disks were weighed and placed in a glass vial containing 10 ml of 0.1 M pH 7.4 phosphate buffer and incubated at 37°C. Aliquot samples of 100 µl were picked out at various time intervals, and replaced by an equal volume of fresh buffer. Absorbance was measured at 565 nm using a Hitachi U-3300 spectrophotometer. The quantity of SR contained in each piece (top and sublayer) was calculated as the total SR added to the polymer solution before lyophilization divided by the weight of the incubated piece.

2.4. In vitro degradation

Foam samples (W_0 ≈ 100 mg) were sterilized by UV exposure under a laminar flow for 30 min and suspended under aseptic conditions in pre-filtered (0.22 µm porosity) phosphate buffer saline (PBS, 2 M, pH 7.4) containing Tween 80 (0.1%) and sodium azide (0.02%). They were incubated at 37°C under a slow tangential agitation. Degradation was followed for a period of 54 weeks. Samples were removed at regular time intervals, rinsed twice with distilled water, surface wiped and weighed (W_s). The samples were then freeze-dried overnight and weighed again (W_r).
Water absorption (WA%) and weight loss (WL%) were calculated according to the following equations:$WA(\%) = 100 \times (W_s - W_0)/W_0$ $WL(\%) = 100 \times (W_0 - W_r)/W_0$.
Water absorption in the short term was used to characterize the wettability of the different foams.
Changes in molecular weight and polymolecularity of the polymers were analyzed by SEC in chloroform with three Ultrastyragel columns (HR1, HR3, and HR4) and a PL-gel precolumn (5µm, HP). The universal calibration curve was established with polystyrene (PS) standards (Polymer Laboratories Ltd., Church Stretton, Shropshire, UK) and the appropriate viscometric equations for PS and PDLLA.
Thermal properties of PDLLA-PELA were investigated by DSC (Thermal Analyst 2100; TA Instruments Inc., New Castle, DE, USA) calibrated with indium. The samples (5-10 mg) were heated under dry, oxygen-free nitrogen, from 0 to 100°C at a rate of 10°C/min. The glass transition temperature (T_g) was measured during the second heating run after quenching of the sample from the melt.

2.5. In vivo implantation

PDLLA containing 10wt% of the PELA copolymer was dissolved in dioxane. This mixture was loaded with

acidic fibroblast growth factor (a-FGF) as follows: 50 μg of a-FGF (PreproTechEC Ltd., London) was reconstituted in 500 μg of PBS containing 10 mg of bovine serum albumin (BSA, Sigma, St Louis, MO, USA). The solution was homogenized, frozen and then lyophilized overnight. The lyophilized protein was ground into a very fine powder, which was dispersed in the polymer solution. The suspension was then freeze-dried as previously described.
Five mm length and 0.5 mm diameter rods were cut out from the sublayer of the foam, parallel to the macro-pore orientation. They were sterilized by UV exposure for 30 min, and soaked into a laminin aqueous solution for one hour. Adult Wistar rats *(n* = 20) were anesthetized. A laminectomy was performed at the thoracic level (vertebra T6-T8) and a
8 mm long longitudinal incision of the dura-mater was realized with a special care to respect the border for the later suture. Hereafter the cord was transected completely and a 3 mm-long tissue segment was removed. Fourteen to twenty polymer rods were carefully aligned to fill the cavity, which had been cleaned and in particular freed from blood contamination. Four to five layers of rods were superimposed, each layer containing 3-4 rods. Between each polymer layer, a-FGF containing fibrin-glue was added in order to stabilize the polymer construct. The interface between the polymer rods and the spinal stumps was also filled with glue. The dura-mater was carefully sutured with a 10/0 nylon suture, in order to maintain the implant in its original position.

2.6. Histology, immunohistochemistry and microscopic analysis

The rats were kept alive from 7 days to 12 weeks. After a lethal injection of Nembutal, rats were perfused intra-cardiacally with paraformaldehyde (4% solution in PBS). For immunohistochemical studies, the spinal cord was removed and fixed in 4% (wt/v) paraformaldehyde solution for 24 h, followed by immersion in 50% sucrose solution for 24 h. 40 μm thick horizontal sections were prepared on a cryostat for immunostaining using the following antibodies: Glial Fibrillary Acidic Protein (GFAP) (Dakopatts, Glostuys, 1/2000), neurofilament protein (NF)-200kDa (Boehringer Mannheim, 1/1000), the low affinity nerve growth factor receptor (NGFr) provided by Dr G. Brook (1/100) and laminin (Sigma, 1/500).
Four polymer rods explanted after 15 days were observed by environmental SEM (ESEM) (Philips XL30 ESEM®). The spinal cords containing the polymer implant were fixed in paraformaldehyde and stored in PBS. The implants were dissected along the long axis of the spinal cord, and the longitudinal sections were observed in wet atmosphere.

3. Results

3.1. SEM morphology and in vitro release study

Micrographs of longitudinal sections of SR-loaded porous foams show two distinct zones with different pore size and morphology (Fig. 1a). The top layer of the foams (1 mm thick) is more porous and less organized than the sublayer, which shows a remarkable orientation of 100 μm macropores along the cooling direction (Fig. 1b). Transversal section of the sublayer shows periodic clusters of 50 μm diameter pores (Fig. 1c), whatever the foam formulation. At higher magnification small (diameter ca. 5-10 μm) spherical particles of SR can be seen trapped within the porous network (Fig. 1d). When SR is dispersed in the polymer solution (A_{dis}) rather than dissolved in it, a skin is formed at the surface of the top layer, which is not the case for the two other foams.
The release profiles of SR from the PDLLA and the PDLLA-PELA mixed foams are shown in Fig. 2. Data are compared for the top layer (a) and the sublayer (b).
The release from the top layer of the mixed PDLLA/ PELA foam shows a burst in the first 5 h of incubation (70wt%). SR release from the top layer of the two PDLLA foams shows a very limited burst, which does not exceed 20% (A_{dis}) and 30% (A_{sol}). The SR release is faster from foam A_{sol} compared to foam A_{dis}, probably as a result of the skin on the surface of foam A_{dis}. Similarly to the top layer, SR release from the sublayer of foam B is faster than from the two other foams, with a higher burst (ca. 50%) in the first hours.

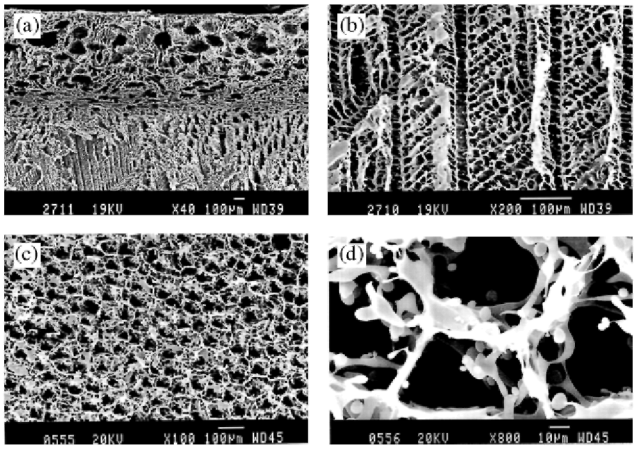

Fig. 1. SEM micrographs of SR-loaded PDLLA-PELA foams. View of the top and the sublayer of the longitudinal section (a), longitudinal orientation of the sublayer pores (b), transversal section in the sublayer at low (c) and high (d) magnification.

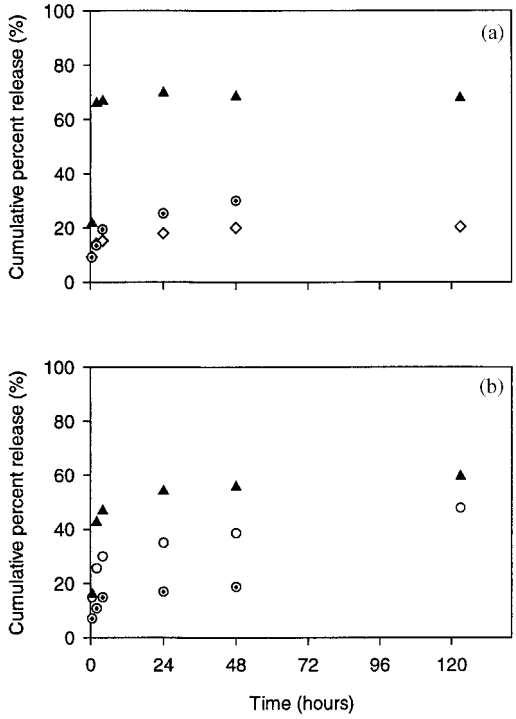

Fig. 2. In vitro cumulative release of SR: dispersed in the PDLLA (A) foam (○), solubilized in the PDLLA (A_{sol}) foam (⊙) and solubilized in the PDLLA-PELA (B_{sol}) foam (▲), (a) Top layer and (b) sublayer of the foams.

At constant porosity and composition, SR is released more rapidly when previously dispersed (A_{dis}) rather than solubilized (A_{sol}) in the polymer solution. In case of solubilization, SR is more intimately embedded into the polymer matrix and a large part of it is released only when the matrix is degraded, so for longer incubation times. All the curves tend to a plateau value, which decreases from the foams B_{sol} to A_{dis} and A_{sol}. As a rule, the SR release is higher from the top layer than from the sublayer, in relation with a larger porosity, as confirmed by SEM observation.

3.2. Wettability of the PDLLA-PELA mixed foams

Fig. 3 compares the amount of water absorbed by the foams over 24 h of incubation. Expectedly the ability to absorb water increases with the PELA content during the first hours of incubation. The foams containing 5 and 10wt% copolymer show an initial burst of ca. 500 wt% of absorbed water, then reach a plateau value, which is higher for the 10 wt% copolymer content. At this composition, the foam sinks to the bottom of the flask, in contrast to the other foams of lower PELA contents. The water absorption is much lower (≤ ca. 200 wt%) when

the copolymer content is 1 wt% or less.

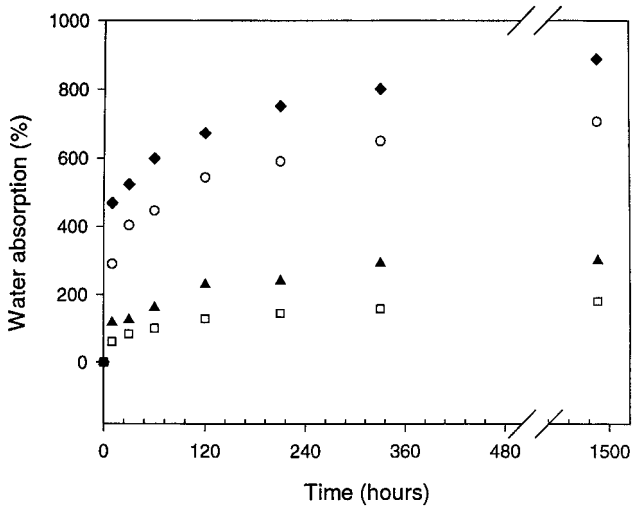

Fig. 3. Water absorption of PDLLA (□) and PDLLA-PELA (1 wt% ▲, 5wt% O, and 10wt%♦) foams versus incubation time.

3.3. In vitro degradation in the long term

Water absorption was found to depend strongly on the PELA content, during the first hours of incubation (Fig. 3). However, over a longer period of time (from 4 weeks to 58 weeks), water absorption reaches an equilibrium value which corresponds to ca. 1000% of WA for all the foams (data not shown), the water absorption increasing much more rapidly when 10 wt% PELA are used. In the absence of PELA (or at low content), the water absorption remains constant from week 7 to one year.
As shown in Fig. 4, all the polymer foams rapidly lost about 10% of their weight, then the weight remained constant until ca. week 19, beyond which it started to decrease at a rate related to the copolymer content. Once again, the foam containing 10 wt% PELA shows a drastic weight loss from week 26 leading to ca. 40% loss after 55 weeks. In the case of foams loaded with 1 and 5 wt% PELA, both the rate of weight loss and the final weight loss are lower. For the pure PDLLA foam, the weight does not change to a large extent and the final weight loss does not exceed 10% of the initial weight.
The change in the pH of the buffered aqueous medium is very small and quite similar for all the foams. Small differences are observed beyond ca. 45 weeks, in relation to the copolymer content. The larger variation in the pH is reported for the higher copolymer content (10wt%). Nevertheless, the pH modification, even in this case, is less than 1 pH unit at the very end of the incubation period (58 weeks).

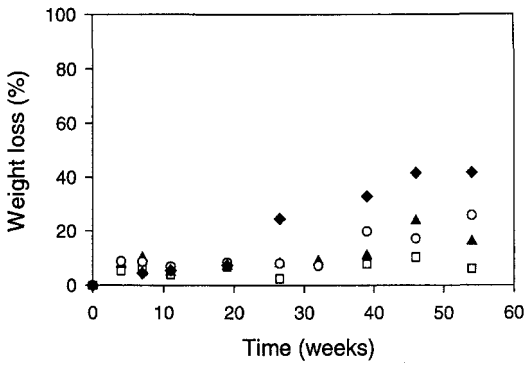

Fig. 4. Weight loss of PDLLA (□) and PDLLA-PELA (1 wt% ▲, 5 wt% O, and 10 wt%♦) foams versus incubation time.

Published in: Biomaterials (2001), vol. 22, iss. 10, pp. 1137-1146
Status: Postprint (Author's version)

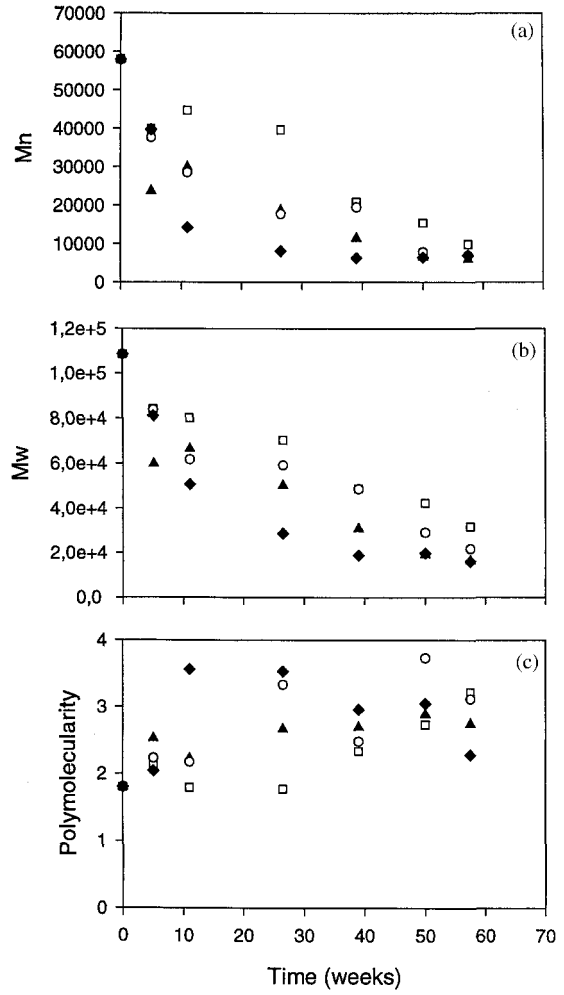

Fig. 5. Changes in number and weight average molecular weight (a and b, respectively) and in polymolecularity (c) versus the incubation time for PDLLA(□) and PDLLA-PELA (1 wt% ▲, 5wt % O, and 10 wt% ♦) foams.

Fig. 5 shows how the number and weight average molecular weights (Figs. 5a and b, respectively) and the PDLLA chain polymolecularity (Fig. 5c) change with time. With 10wt% PELA, both the M and M drop down to 25% of the original value after 11 weeks, compared to ca. 50% in case of 1 and 5 wt% PELA and 80% for the unmodified PDLLA.
At week 50, M_n of the three PDLLA-PELA foams is similar (ca. 7000) but much lower than M_n of pure PLA. At a certain incubation time (i.e. week 11), the largest polymolecularity (3.5) is observed for the 10wt% PELA loading.

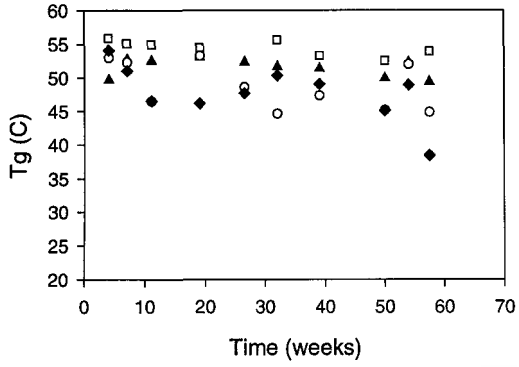

Fig. 6. Time dependence of T_g for the PDLLA(□) and PDLLA-PELA (1 wt% A. 5wt% O, and 10wt%♦) foams on the incubation time.

Published in: Biomaterials (2001), vol. 22, iss. 10, pp. 1137-1146
Status: Postprint (Author's version)

The DSC thermogram for the four foams shows an endothermic peak at ca. 50°C during the first heating run, which completely disappears after heating above the glass transition temperature (T_g) (thus for the second heating run). At the beginning, T_g for all the foams was ranging between 50 and 57°C, and was not significantly influenced by PELA. No sign of PEO crystallization and melting, known to be observed around 60°C, is observed whatever the copolymer content and the incubation time. The dependence of T_g on the incubation time is shown in Fig. 6. A significant decrease in T_g is observed only for foams containing at least 5wt% of copolymer, for incubation time longer than 40 weeks.

3.4. In vivo observations

After 7 days, the examination of the transplanted area shows that the porous PDLLA-PELA rods are completely integrated within the spinal tissue. The polymer rods bridge the gap between the proximal and the distal spinal stumps, resulting in a improved resistance to mechanical deformation. One month later, the polymer is perfectly integrated within the host, with a restored anatomic continuity. The transplanted area appears slightly translucent as compared to the adjacent normal nervous parenchyma. The implant remains flexible enough to accommodate the rachis motion, which can deform the spinal-polymer interface.

3.5. *Histological observations*

After 13 days of implantation, the histological analysis of the transplanted area confirms that the polymer rods are still properly orientated along the spinal axis (Fig. 7a). The polymer is perfectly integrated in the spinal cord. It is localized at the center of the lesioned site and two transition zones of a few hundreds μm length are observed, which establish the connection between the implant and the neural tissue.

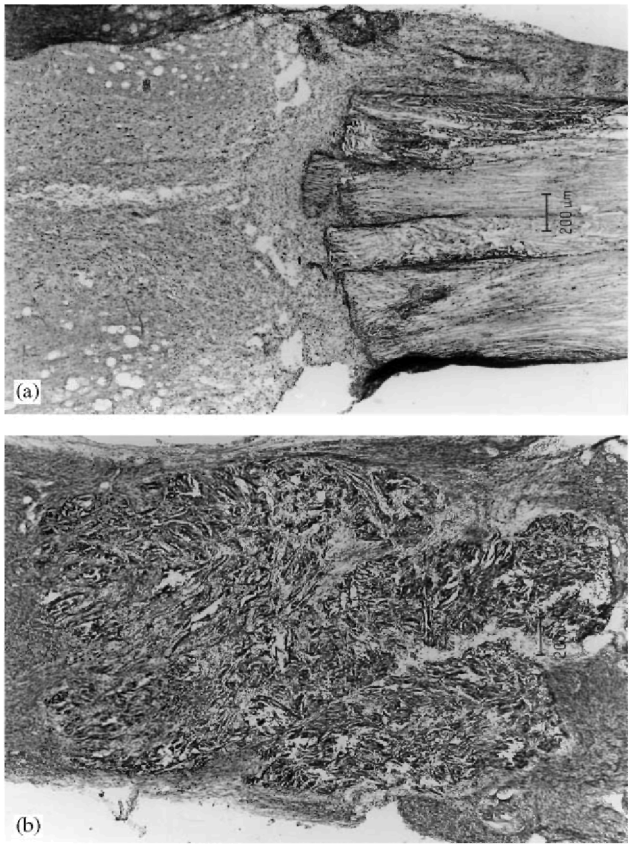

Fig. 7. Low magnification view of polymer rods implanted in the resected spinal cord. Hematoxylin-eosin staining. (a) 13 days of survival: longitudinal orientation of the polymer rods in the resected area. The cellular invasion is moderate. (b) 30 days of survival: numerous cells have invaded the polymer rods.

In a few animals, the polymer rods are surrounded by a mono- or multicellular layer, giving the appearance of a barrier to further cell penetration (Fig. 7a). One month after the implantation, a massive cellular invasion has occurred following the longitudinal orientation of the polymer rods (Fig. 7b). Many cells are found to penetrate the transplant but the vast majority of them is localized in the space between the adjacent polymer rods.

Published in: Biomaterials (2001), vol. 22, iss. 10, pp. 1137-1146
Status: Postprint (Author's version)

3.6. Immunohistochemical observations

At 1 month of implantation, GFAP-positive astrocytes are observed in the adjacent spinal tissue and in the two transition zones but conversely, only few astrocytes penetrate into the polymer implant (Fig. 8a). This suggests that gliosis has developed at the proximal and distal spinal stumps, without further extension into the polymer rod matrix. Immunostaining with anti-NGFr antibody reveals numerous Schwann cells localized both in the transition zones and within the polymer implant (Fig. 8b).

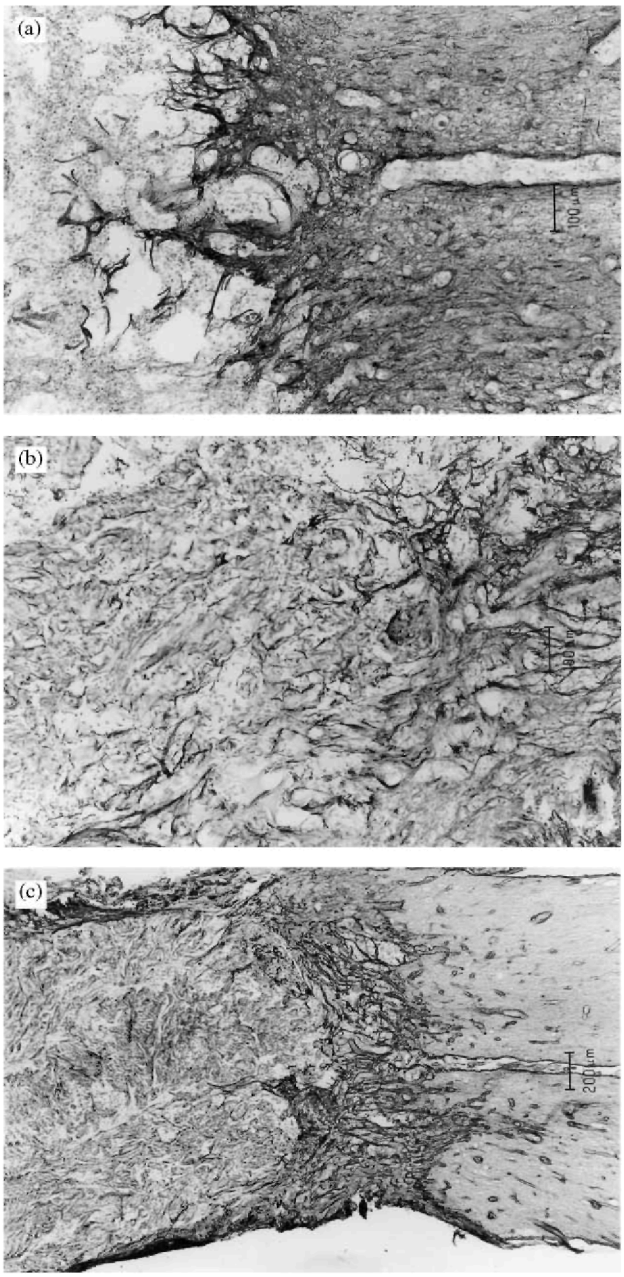

Fig. 8. Immunostaining using GFAP (a), NGFr (b), and laminin (c) antibodies, one month after the implantation. (a) GFAP expression is increased at the two extremities of the resected area. Some astrocytes penetrate the rostral and caudal extremities. They are characterized by cytoplasmic extensions rich in GFAP. The penetration remains limited to the transition zone between the polymer and the spinal tissue, (b) Immunostaining using NGFr antibody demonstrates the presence of Schwann cells. The transition zone is always very rich in Schwann cells that penetrate between adjacent polymer rods following their longitudinal orientation. Schwann cells are also observed inside the polymer. (c) Immunostaining using laminin antibody shows the presence of Schwann cells and endothelial cells in the transition zone.

Schwann cells progress from the transition zones to the space between the adjacent polymer rods and grow along these longitudinal pathways over the whole length. Some Schwann cells are also found to penetrate the macrochannels but not extensively. They are either isolated or, more frequently, they form long channels orientated along the axis of the spinal cord. They probably migrate from the posterior roots adjacent to the cord resection. Immunostaining for laminin shows an intense immunoreactivity identifying the presence of both Schwann cells and endothelial cells (Fig. 8c). Endothelial cells are either isolated or grouped into new vessels within the polymer construct. As for Schwann cells, endothelial cells show a longitudinal orientation and they are essentially observed in between the polymer rods.
NF-positive profiles are observed within the whole implanted area (Fig. 9a) and particularly in the transition zones (Fig. 9c). They follow a remarkable longitudinal orientation. They are either isolated or assembled into bundles. In the close vicinity of the rods, most of these axons seem to follow the Schwann cell pattern formed in between the rods (Fig. 9d). Some of them also penetrate the lumen of the macropores within the polymer structure itself. Others have deviated at the polymer surface, having grown around a rod. The origin of the axons, for propriospinal or supraspinal contingents, needs to be confirmed by future appropriate neuroanatomical tracing procedures. The continuity of their profiles between the cord stumps and the polymer suggests that they are originating from the cord rather than directly from the adajacent roots. Some of the axons probably originate from the posterior roots in close association with Schwann cells. However, most of them originate from the proximal and distal spinal segments of the sectioned spinal cord.

3.7. ESEM observations

ESEM observations of longitudinal cross-sections of one implanted porous polymer piece are reported in Fig. 10 and illustrate the good integration of the polymer implant in the spinal tissue after 15 days. The polymer is easily identified by its typical porous structure, suggesting that the in vivo implantation does not perturb the original morphology to a large extent. It is clearly covered by various cellular structures that smooth the geometrical contour shapes of the porous matrix. The presence of cellular elements coming from the dura-mater in contact with the polymer confirms the penetration of the implant by cells from the polymer surface (Fig. 10a).

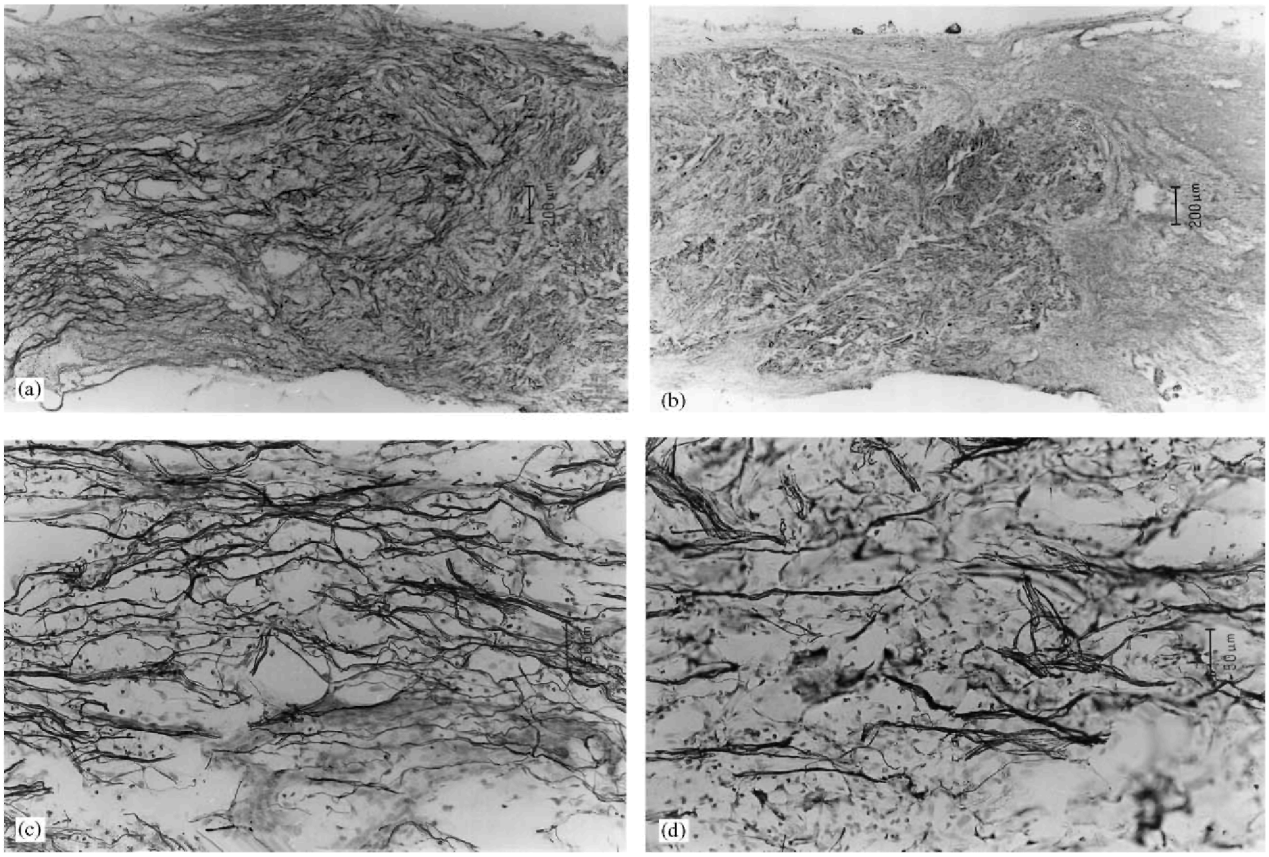

Fig. 9. Immunostaining using NF antibody shows the neuritic invasion in both the resected area and the polymer implant (a) as compared to an adjacent section immunostained without the primary antibody (b). The transition zone (c) is massively invaded by neuritic profiles that extend longitudinally toward the polymer and particularly in between the polymer rods (d). The neurites, either isolated or grouped into bundles, penetrate the polymer along the longitudinal orientation (c).

Published in: Biomaterials (2001), vol. 22, iss. 10, pp. 1137-1146
Status: Postprint (Author's version)

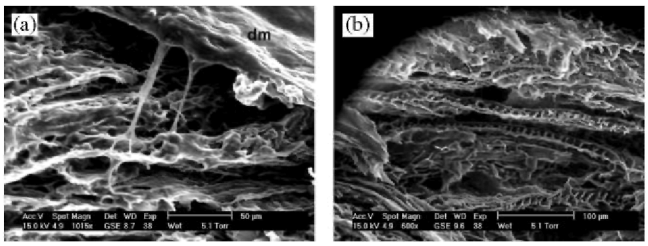

Fig. 10. ESEM observations of the polymer implant. Surface (a) and core (b) of the polymer covered by cellular elements. Some of these cells are originating from the dura-mater (dm).
Few cellular components are observed within the internal porous structure (Fig. 10b). Considering the limitation of this technique, which gives only morphological information, we could not determine precisely the origin and the nature of these cells.

4. Discussion

One of the major challenges in the field of spinal cord repair is to stimulate the regrowth of severed axons and reconstitution of pathways. In this prospect, strategies which combine implantation of artificial scaffolds as supports for tissue ingrowth and local delivery of neuroac-tive growth factors able to accelerate the regeneration process are very promising. The phase separation technique used to prepare the polymer nerve guides takes advantage of the sublimation properties of some organic solvents to create pores within resorbable polyester matrices. As a result, the loading of drugs, proteins or growth factors is feasible with lower risk of activity loss compared to other porogen techniques that require high processing temperatures or the use of porogens to be leached out [4]. In this work, SR, with solubility of 20 mg/ml in water, has been chosen in a first approach to mimic short peptides, such as angiotensin and chemotac-tic agents. Release of SR and phosphatase alkaline (AP) from porous foams made of poly(L-lactide) of various weight average molecular weights (PLLA of 500,000, 130,000, and 2000) was previously studied by Lo et al. [5]. In their study, foams were produced by freeze-drying from molten naphthalene and phenol solutions. However, some loss of AP activity was reported due to the relatively high melting temperature (T_m) of the selected solvents (25% of AP activity was lost). The lower T_m of dioxane (11°C) makes it a more suitable candidate for persistence of the drug bioactivity although this solvent is reported as carcinogenic. Other solvents with similar properties but less toxicity have been identified during the course of this research as will be published elsewhere. This work paid attention to the influence of the pore microstructure and the foam wettability on the release of SR incorporated into PDLLA foams either by dispersion or by dissolution in the polymer solution, before freeze-drying. Addition of a PDLLA-b-PEO copolymer is favorable to a rapid water absorption, which improves the wettability of the PDLLA foams and their handling for the in vivo implantation as well. Consequently, the kinetics of the SR release is faster from the PDDLA-PELA (10wt% PELA) foams as compared to pure PDLLA foams, at similar pore microstructure. For the sake of comparison, static contact angle measurements of distilled water have been performed on polymer films to measure the hydrophilicity of the film surface. Results show that the contact angle decreases when the copolymer content is increased up to 25 wt% (personal results).
Modification in the pore surface microstructure has also consequences on the kinetics of the SR release. The surface of the PDLLA foam A_{dis}, in which SR is dispersed rather than dissolved, is covered by a skin which delays the SR release compared to the more porous surface of the foams A_{sol} and B_{sol}. The addition of SR aqueous solution to the polymer solution before freeze-drying at least partly explains this difference in the surface topography. SR is released faster when dispersed rather than solubilized in the polymer matrix. It is thus possible to modulate the release of bioactive molecules by the appropriate control of the pore microstructure and wettability of the foams, and by the method of incorporation.
Degradation time is another major issue in spinal tissue engineering when biodegradable porous scaffolds are used. The onset of degradation should not occur before the regenerated nerve fibers are mature enough to be self-supporting but have to take place as soon as this scaffold is no more useful. Although many studies were devoted to the in vitro and in vivo degradation of poly-lactide-based devices, the degradation time is difficult to predict because of the complex influence of the characteristic features of the device (size, shape, porosity) and the variability of the experimental parameters (composition of the in vitro medium, site of in vivo implantation). This study shows that the addition of an amphiphilic PELA copolymer increases the degradation rate of the PDLLA porous foams. After 18 weeks of incubation in water, the weight loss increases more rapidly for the foam containing 10wt% copolymer in relation to high water absorption. As a result, the polymer foams swell, the distance between the polymer chains increases and the material becomes more permeable. The increased water absorption is potentially beneficial in our paradigm, since it provides a wet environment devoid of any gas entrapment persisting into the pores of the polymer foam. It is also favorable to the rapid diffusion of biological

fluids and growth factors, either previously incorporated into the foam and/or secreted in situ by cells. Lastly it also stimulates the hydrolytic degradation mechanism. Accordingly, M_n and M_w of the PDLLA chains decrease much more rapidly in 90/10 PDLLA-PELA foam than in pure PDLLA foam. Moreover, Grizzi et al. have showed that degradation of large size PLA/GA devices was size-dependent and degraded het-erogeneously, the degradation being faster in the internal part than at the surface because of the accumulation of carboxylic acid end-groups in the matrix [6]. This effect was not observed for the degradation of the PLA-PELA porous foams, more likely because of the high and open porosity that may facilitate the release of leachable oligomeric degradation products. Recently, Gautier et al. reported that the in vivo degradation profile for PLA and PLGA cylinders implanted in the rat spinal cord was similar to that one observed in vitro [7].
The 90/10 PLA-PELA foam was selected for in vivo study because of the enhanced wettability and degradation rate. The transection of the spinal cord alters the cellular environment at the site of the lesion and interrupts the ascending and descending axonal tracts, so resulting in permanent paraplegia. Since the experiments of Aguyo demonstrating the regrowth of propriospinal axons into sciatic nerves from adult rats bridging a cord transection [8], the dogma of the absence of adult CNS regeneration has been challenged. Many different types of material have been studied for their capacity to enhance repair of the lesioned spinal cord by e.g. the interposition of acellular materials: extracellular matrix, collagen grafts [9,10], carbon filaments [11], tubes of polyacrylonitrile-polyvinylalcohol (PAN-PVC) [12], homo- and heterogeneous methacrylate-derived porous hydrogels [13], and nitrocellulose membranes [14]. The incorporation of Schwann cells and/or growth factors within the guidance channels was always reported to be beneficial [15-20]. Major progress in CNS regeneration was recently reported as result of a multilateral approach based on peripheral nerve grafts in conjunction with acidic fibroblast growth factor containing fibrin-glue to bridge a spinal cord lesion in rat [21]. The success of this strategy might originate from several key features: (i) the precise orientation of the peripheral nerve fragments, (ii) the strong bonding of the nerve fragments and the spinal cord stumps by fibrin glue containing a-FGF, (iii) the immobilization of the dorsal spine by a metallic hopping. That is the reason why we incorporated laminin on the surface of the polymer which has also been embedded in fibrin-glue containing a-FGF. Moreover, this study highlighted the importance of the three-dimensional organization of the spinal reconstruction device. According to this, we implanted longitudinally orientated porous PLA rods. Moreover, previous experiments in the PNS [3] demonstrated that the surface of these polymer rods is the most favorable milieu for the axogenesis. With this in mind, we implanted a multilayer PLA construct in the transection area, rather than a single thicker block in order to fill in the spinal cavity, with the expectation to increase the polymer surface area. Interestingly, the inter-rods phase is composed of fibrin glue with the same longitudinal orientation than the pores of the PLA foam. There are only few reports on the regeneration through fully synthetic materials rid of cellular components. In our opinion, the success of these reconstruction strategies relies upon: (i) the biocompatibility and the resorbability of the material, (ii) its rapid integration in the host tissue depending on e.g. the polymer properties and wettability, and (iii) the three-dimensional orientation of the guiding structure and the available surface for cellular migration and neoaxogenesis.

5. Conclusions

This study has shown that the parallel assembly of rods of porous PLA containing an amphiphilic PLA-b-PEO copolymer is a promising strategy to bridge a defect in the spinal cord of adult rats. This type of multicompo-nent synthetic implant promotes cell infiltration, an-giogenesis and allows important neuritic growth by recruiting cells and axons from the host tissue. The exact origin of these axons needs to be determined by im-munohistology and by anterograde and retrograde tracing. The spinal cord continuity can be restored, the synthetic polymer being intimately integrated into the host tissue. The PELA copolymer provides the PLA foams with a higher wettability and swelling capacity, and accordingly favors the transport of nutrients and fluids through its porous network. As a result, it modulates the biological processes through the control of the diffusion of growth factors that can be previously incorporated into the foams but also naturally secreted after injury.

Acknowledgements

CERM is indebted to the "Services Fédéraux des Affaires Scientifiques, Techniques et Culturelles" (SSTC) for financial support in the frame of the "Pôles d'Attraction Interuniversitaires: Chimie et Catalyse Supramoléculaire". The authors acknowledge Dr G. Brook (RWTH, Aachen) for providing NGFr antibody. V.M. is grateful to Dr J. Coudane, at the C.R.B.A, University of Montpellier (France) for helpful assistance in ESEM.

References

[1] Schugens C, Maquet V, Grandfils C, Jérôme R, Teyssié P. Biodegradable and macroporous polylactide implants for cell transplantation: 1. Preparation of macroporous polylactide supports by solid-liquid phase separation. Polymer 1996;37:1027-38.
[2] Schugens C, Maquet V, Grandfils C, Jérôme R, Teyssié P. Poly-lactide macroporous biodegradable implants for cell transplantation. II. Preparation of polylactide foams by liquid-liquid phase separation. J Biomed Mater Res 1996;30:449-61.
[3] Maquet V, Martin D, Malgrange B, Franzen R, Schoenen J, Moonen G, Jérôme R. Peripheral nerve regeneration using bioresorbable macroporous polylactide scaffolds. J Biomed Mater Res 2000;52:639-51.
[4] Maquet V, Jérôme R. Design of macroporous biodegradable polymer scaffold for cell transplantation. In: Porous materials for tissue engineering, vol. 250. Uetikon-Zuerich: Trans Tech Publications Ltd, 1997. p. 15-42.
[5] Lo H, Kadiyala S, Guggino SE, Leong KW. Poly(L-lactic acid) foams with cell seeding and controlled-release capacity. J Biomed Mater Res 1996;30:475-84.
[6] Grizzi I, Garreau H, Li S, Vert M. Hydrolytic degradation of devices based on poly(DL-lactic acid) size-dependence. Biomater 1995;16:305-11.
[7] Gautier SE, Oudega M, Fragoso M, Chapon P, Plant GW, Bunge MB, Parel J-M. Poly(α-hydroxyacids) for application in the spinal cord: resorbability and biocompatibility with adult rat Schwann cells and spinal cord. J Biomed Mater Res 1998;42:642-54.
[8] Aguayo AJ, David S. Axonal elongation into PNS "bridges" after CNS injury in adult rat. Science 1981;214:931-3.
[9] Marchand R, Woerly S, Bertrand L, Valdes N. Evaluation of two cross-linked collagen gels implanted in the transected spinal cord. Brain Res Bull 1993;30:415-22.
[10] Joosten EAJ, BaKr PR, Gispen W-H. Collagen implants and cor-tico-spinal axonal growth after mid-thoracic spinal cord lesion in the adult rat. J Neurosci Res 1995;41:481-90.
[11] Khan M, Griebel R. Carbon filament implants promote axonal growth across the transected rat spinal cord. Brain Res 1991; 541:139-45.
[12] McCormack M, Goddard M, GueHnard V, Aebisher P. Comparison of dorsal and ventral spinal root regeneration through semipermeable guidance channels. J Comput Neurol 1991;313:449-56.
[13] Woerly S, Pinet E, De Robertis L, Bousmina M, Laroche G, Roitback T, Vargova L, Sykova E. Heterogeneous PHPMA hydrogels for tissue repair and axonal regeneration in the injured spinal cord. J Biomater Sci Polym Edn 1998;9: 681-711.
[14] Houle J. Regeneration of dorsal root axons is related to specific non-neuronal cells lining NGF-treated intraspinal nitrocellulose implants. Exp Neurol 1992;118:133-42.
[15] Guest J, Rao A, Olson L, Bunge M, Bunge R. The ability of human Schwann cell grafts to promote regeneration in the transected nude rat spinal cord. Exp Neurol 1997;148:205-522.
[16] Xu X, GueHnard V, Kleitman N, Bunge M. Axonal regeneration into Schwann cell-seeded guidance channels grafted into transected adult rat spinal cord. J Comput Neurol 1995;351:145-60.
[17] Xu X, Chen A, GueHnard V, Kleitman N, Bunge M. Bridging Schwann cell transplants promote axonal regeneration from both the rostral and caudal stumps of transected adult rat spinal cord. J Neurol 1997; 26:1-16.
[18] MacDonald RT, McCarty SP, Gross RA. Enzymatic degradabil-ity of poly(lactide): effects of chain stereochemistry and material crystallinity. Macromolecules 1996; 29:7356-61.
[19] Oudega M, Hagg T. Nerve growth factor promotes regeneration of sensory axons into adult rat spinal cord. Exp Neurol 1996; 140:218-29.
[20] Oudega M, Xu XM, Guenard V, Kleitman N, Bunge M. A combination of insulin-like growth factor I and platelet-derived growth factor enhances myelination but diminishes axonal regeneration into Schwann cell grafts in the adult rat spinal cord. Glia 1997; 19:247-58.
[21] Cheng H, Cao Y, Olson L. Spinal cord repair in adult paraplegic rats: partial restoration of hind limb function. Science 1996; 273:510-3.